

**Western Indian Ocean Regional geo-spatial data on climatic drivers of change (DoC's)  
in marine ecosystems**

Data documentation

Prepared for ASCLME by

Joseph M. Maina

30-Nov-2011

## **Background**

The overall objective of this project is to develop specific spatial data products at regional scale, for the coastal and/or marine areas of all the western Indian Ocean countries, including South Africa, Mozambique, Tanzania, Kenya, Somalia, Comoros, Seychelles, Madagascar, Mauritius and France. This report summarizes the data products, which have been prepared, on the basis of their relevance to the Large Marine Ecosystems (LME's). The preparation of these data products involved retrieval from various sources, spatial analysis and modelling, and scaling. Effort has been made to standardize various data properties including spatial extent and formats.

These data include ocean climate related parameters including sea surface temperature, precipitation, wind velocity and the ultraviolet radiation; geomorphological parameters including the coastal watersheds and soil loss estimates and river discharge; ocean geophysical parameters including ocean colour and substances data (Chlorophyll a, Colored Dissolved Organic Matter and total suspended solids); and the coral and mangroves exposure to the drivers of change. The later two are a product of spatial modelling incorporating some of the data also included here. The spatial extent for the data does vary but as much as possible an effort was made to cover the western Indian Ocean continental and the island countries.

Here I briefly describe the data, the analysis and modelling procedures. Key citations for the data are provided. In addition, a spreadsheet with metadata has been prepared alongside this report. The naming convention is consistent, with the first letter (O, L, or M denoting Ocean, Land and Marine respectively, and the second letter (C=climate, G=geomorphological, E=Ecosystems, and M=management) denoting the data class.

## Table of contents

---

	<b>Page</b>
Product LG01: Coastal Susceptibility to Erosion	5-7
LG01a: Rainfall erosivity	
LG01b: Soil data	
LG01c: Elevation data	
LG01d: Slope/Relief complexity	
LG01e: Coastal Watersheds	
Product LG02: River discharge (runoff)	7
Product LG03: Current Land cover land use map	7
Product LG04: Future Land cover land use map	8
Product OC01: Historical Sea surface	8
OC01a: Time series data – 1982-2009	
OC01b: Maximum SST based on LC01a	
OC01c: Minimum SST based on LC01a	
OC01d: SST variability (standard deviation) based on LC01a	
OC01e: Mean SST based on LC01a	
Product OC02: Projected sea surface temperature	8
OC02a: Time series GFDL SST for the three SRES scenarios	
OC02b: Future SST anomalies based on a 1950-2000 SST baseline	
Product OC03: Tides (FES 2004 tide ranges and variability)	8
OC03a: Weekly tidal maximum, minimum and average time series	
OC03b: Average maximum tide computed from LC03a	
OC03c: Average minimum tide computed from LC03a	
OC03d: Average tidal range computed from LC03a	
Product OC04: Case 1 and Case 2 [Chlorophyll, TSM and CDOM]	10
OC04a: Time series - merged case I & II chlorophyll, CDOM and TSM	
OC04b: Average Chlorophyll based on OC04a	
OC04c: Average TSM based on OC04a	
OC04d: Average CDOM based on OC04a	
<b>Product OC05: Ocean acidification</b>	
Product OC06: UV 290-300nm	12
LC01: Projected rainfall under IPCC SRES	13
LC01a: CNRM model time series for A1b, A2, and B1	

LC01b: NCAR model time series for A1b, A2, and B1	
LC01c: GISS model time series for A1b, A2, and B1	
OC07: Wind velocity and Doldrum Index	14
OC07a: Long term wind velocity magnitude (windiness)	
OC07b: Long term high wind velocity (>3m/s) duration	
OC07c: Doldrum index, as a function of OC07a and OC07b	
LE01: Mangrove exposure to DoC	13
LE01a: exposure to steep slope (calculated from LG01e)	
LE01b: Watershed susceptibility to erosion (same as LG01a)	
LE01c: Mangrove ecological condition (Average NDVI)	
LE01d: Human pressure index	
LE01e: Land Development Intensity index	
LE01f: Exposure to land development and erosion	
LE01g: Exposure to sea level rise	
LE01h: Mangrove exposure map	
LE02: Mangrove extent and NDVI time series	16
LE02a: Mangrove-NDVI time series (Monthly averages from 2000-2011)	
LE02b: Mangrove extent shape-files for East Africa and Madagascar	
LE02c: Mangrove extent – Giri et al. Global	
ME01: Coral exposure to DOC	17
MM01: ASCLME countries – updated protected area polygons – to incorporate all type of closures e.g. new community closures in TZ, MQ and Kenya	
MM02: Oil, gas and mineral prospecting and exploitation sites	

### List of figures

Figure 1. Figure showing the processing of the standard ocean colour products to enhance measurements for coastal areas.

Figure 2. A flow chart showing the steps and data used to extract and synthesizing the variables into a mangrove exposure map.

### List of tables

Table 1. Summary of variables identified by regional mangrove experts as important drivers of change for mangroves ecosystems and their roles in impacting mangroves

### **Product LG01a: Coastal Susceptibility to Erosion**

Development of land management priorities requires detailed local-level information on sources of sediment, and the vulnerability of areas to erosion. Based on the landscape-wide indicator of the vulnerability of land to soil erosion, developed by the World Resources Institute, a susceptibility to erosion map in the coastal watersheds was developed. It incorporates the slope of the land, soil erodibility, and annual precipitation into a 90 m resolution indicator of the relative vulnerability of the land to erosion (Equation 1). This indicator does not consider the current land cover or land use. Rather, it provides an overall indicator of erosion-prone areas, and therefore, a guide to areas where restrictions on development, or the implementation of best agricultural management practices should be encouraged. This product has been prepared within the context of the management of mangroves, hence the extent covers coastal watersheds in East Africa, Northern and west coast of Madagascar.

Equation 1: Vulnerability of Land to Erosion -  $Vulnerability = R * K * S^{0.6}$

*Where R – Rainfall-runoff erosivity factor K – Soil erodibility factor S – Slope (in degrees)*

**LG01b: Rainfall erosivity** - Rainfall erosivity is a measure of the erosive force of rainfall, and is a required input of Revised Soil Loss Equation (RUSLE). Often, the large-scale rainfall erosivity mapping in data-poor regions is based on interpolation of erosivity values derived from rain gauge data (Vrieling et al. 2000). Indices used to estimate the rainfall erosivity include R-factor (Renard and Freimund 1994); the Fournier Index (FI) and the modified Fournier Index (MFI). MFI was found to provide good spatial estimates of annual erosivity when used with the monthly satellite-based precipitation. Here we provide MFI map published in Vrieling et al. 2000. This map covers all of Africa.

**LG01c: Soil data** - Soil data was obtained from Version 1.1 of the Harmonized soil database of the world (FAO/IIASA/ISRIC/ISSCAS/JRC 2009). Using the soil types in the soil database a soil hydrologic group map for the study area was derived using reclassification procedure; (ii) soil erodibility factor (K- Factor) represents soil's susceptibility to erosion by rainstorms. It is an integrated average parameter based on several different erosion and hydrologic processes. K-factor is expressed as a function of sand, silt, clay and organic carbon concentration, which were derived using reclassification procedures using the soil database. A low K-factor (about 0.05 to 0.2) indicates a high resistance to erosion and a high

K-factor (about 0.4 or greater) indicates easily eroded soil. K was computed using the equation (2).

**Equation 2**

$$K = \left[ 0.2 + 0.3 \exp \left\{ -0.026 SAN \left( 1 - \frac{SIL}{100} \right) \right\} \right] \left( \frac{SIL}{CL + SIL} \right)^{0.3} \left( 1 - \frac{0.25C}{C + \exp(3.7 - 2.9C)} \right) \left( 1 - \frac{0.7SN1}{SN1 + \exp(-5.5 + 22.9SN1)} \right)$$

Where SAN, SIL, CL and C are (%) of sand, silt, clay and organic carbon contents of the soil respectively, SN1=1-SAN/100.

**LG01c: Elevation data-** Digital elevation model (DEM) was downloaded from CGIR website. The DEM is derived from the shuttle Topographic Radar Mission (SRTM). We utilized DEM as an input factor for slope steepness (S), which is a parameter that adjusts erosion rates in the equation for susceptibility to erosion (Equation 1).

**LG01d: Slope/Relief complexity** - Slope in degree was derived from the SRTM digital elevation model using ArcGIS spatial analyst extension.

**LG01e: Coastal Watersheds**

Coastal watersheds were extracted from the freely available 90m horizontal resolution SRTM digital elevation model (DEM). Watersheds were generated from a flow direction map derived from the DEM using ArcInfo spatial analyst extension. The watersheds were then generalized to develop medium sized watersheds which out flow in to the coast.

**Product LG02: River discharge (runoff)**

Gridded fields of long-term average (1950-2000) Annual River discharge data was obtained from the water balance model (Vorosmarty et al., 1998) with improved interception function as recommended by Federer et al. (2003). The University of New Hampshire Water Systems Analysis Group produced this model (<http://www.wsag.unh.edu/data.html>). This data is presented as one annual and 12 monthly climatological river runoff fields. The monthly runoff values are given in mm/mo at 30-minute (0.5 degree) spatial resolution.

**Product LG03: Food and Agriculture Organization (FAO) Land use systems**

Version 1.1 of a thematic grid of Land Use Systems (LUS) and its attributes for Sub-Saharan Africa with a spatial resolution of 5 arc minutes or 0.083333 decimal degrees. This dataset is

developed in the framework of the LADA project (Land degradation Assessment in Drylands) by the Land Tenure and Management Unit of the Food and Agriculture Organization of the United Nations and is copyright of FAO/UNEP GEF. The LUS map implementation is based on a innovative methodology combining more than 10 global datasets. Due to the map generation method, the quality of the map can never be uniform. The overall quality of the map depends heavily on the individual quality of the data for the different countries (<http://www.fao.org/geonetwork/srv/en/>).

**Product LG04: Future Land use / land cover**

LandSHIFT (Land Simulation to Harmonize and Integrate Freshwater Availability and the Terrestrial Environment) is a land use change model for global and regional scale simulation experiments (Schaldach et al. 2011), developed by the The Center for Environmental Systems Research (CESR). Land use map for 2050 based on (a) markets first, and (b) sustainability first scenarios, and were derived from the landSHIFT model. Land cover maps for Africa were at 5 arc-minutes spatial resolution. Documentation of these maps and scenarios can be found in Schaldach et al. 2011; Alcamo et al. 2011.

**Product OC01: Historical Sea surface temperature** - Sea surface temperature derived variables were obtained from the second version of the coral reef temperature anomaly database (CoRTAD) (Selig et al. 2010). This database contains global SST and related thermal stress metrics at an approximately 4-km resolution weekly from 1982 through 2008, derived from measurements from the Advanced Very High Resolution Radiometer on board NOAA suite of polar orbiting satellites. The global accuracy of the retrieval algorithm based on comparisons with in situ buoys indicates values of 0.02 - 0.5°C (Kilpatrick et al 2001). When compared with in situ temperature from data loggers at shallow depth in the western Indian Ocean, RMSE of 0.87°C were reported (Selig et al. 2010). The CoRTAD reanalysis database has also been evaluated using *in situ* observations from different coral reef locations globally and at depths ranging from 0-9m, which corresponds to depths of most coral reef habitats (Selig et al. 2010). This evaluation reported RMSEs ranging from 0.49 - 0.81 °C, and a coefficient of determination ( $R^2$ ) of 0.72 - 0.96 (Selig et al. 2010). Overall, the performance of this data for global, regional and subregional coastal applications is adequate, notwithstanding the fact that radiometers measure the temperature at the sea surface while most *in situ* measurements are based on bulk temperature at shallow depths. Data were extracted and the aggregations below performed.

**OC01a:** Time series data – 1982-2009

**OC01b:** Maximum SST based on LC01a

**OC01c:** Minimum SST based on LC01a

**OC01d:** SST variability (standard deviation) based on LC01a

**OC01d:** Mean SST based on LC01a

**Product OC02: Projected sea surface temperature** - Historical sea surface temperature time series data (and derived variables) were extracted from the respective sources. AOGCM (atmospheric-ocean global circulation models) will be downloaded from the Geophysical Fluid Dynamics Laboratory (GFDL) website, for all the following IPCC scenarios: A1B [720ppm], A2 [870ppm] and B1 [550ppm]. Sea surface temperature anomalies based on these scenarios were computed, as a proxy for the predicted thermal stress on coral reefs.

**OC02a:** Time series GFDL SST for the three SRES scenarios

**OC02b:** Future SST anomalies based on a 1950-2000 SST baseline

**Product OC03: Tides (FES 2004 tide ranges and variability)** - Over the last decade, the tidal research group of Le Provost and collaborators have produced a series of finite element solution (FES) tidal atlases; FES-2004 is the latest release. Data are computed from the tidal hydrodynamic equations and tide gauges and altimeter data assimilation (Le Provost et al. 1998). When cross validated with other tidal products, the FES-2004 atlas was found to be the most accurate, with improved performance in shelf and coastal areas and moderately deeper areas (Le Provost et al. 1998, Lyard et al. 2006). The accuracy of the 15 tidal components used in the model ranges from 2-12cm and varies by region (Lyard et al. 2006). Therefore, local applications would require calibration with tidal observations at the same scale.

The digital FES-2004 tidal model and the associated extraction software were downloaded from the Laboratoire d'Etudes en Géophysique et Océanographie Spatiales website (<http://www.legos.obs-mip.fr/en/soa>) (Le Provost et al. 1998, Lyard et al. 2006). The software in C++ was modified to enable gridding of the tidal predictions for a user defined spatial and temporal extents. To minimize the computer processing time, the model's temporal resolution was degraded from hourly to 6-hr interval. These predictions were then aggregated for average, minimum, and maximum heights over seven day intervals and gridded at the model's spatial resolution of roughly 14-km. To capture the long-term conditions and variability, the model was run for 8 years from 1987 with a three-year

interval, including 1987, 1990, 1993, 1996, 1999, 2002, 2005, and 2008. Tidal ranges were computed as the long term averaged difference between the weekly maximum and minimum simulated tidal heights.

**OC03a:** Weekly tidal maximum, minimum and average time series for 1987, 1990, 1993, 1996, 1999, 2002, 2005, and 2008

**OC03b:** Average maximum tide computed from LC03a

**OC03c:** Average minimum tide computed from LC03a

**OC03d:** Average tidal range computed from LC03a

**Product OC04: Case 1 and Case 2 [chlorophyll, TSM and CDOM]** - Oceanic satellite observations in the visible and near-infrared bands allow for the measurement of a variety of ocean colour information including phytoplankton chlorophyll-*a*, total suspended matter (TSM), and colored dissolved organic matter (CDOM) (Morel and Prieus 1977, Morel and Belanger, 2006). For modelling purposes, ocean waters are commonly described as being of Case I or case II types (Morel and Prieus 1977, Morel and Belanger, 2006). The former type are those waters whose optical properties are determined primarily by phytoplankton and related colored dissolved organic matter (CDOM) and detritus degradation products; while the later represents the turbid coastal zones influenced by land drainage or sediment re-suspension, with optical properties mainly influenced by CDOM of terrestrial origin, mineral particles, various suspended sediments, urban discharges and industrial wastes (Morel and Prieus 1977).

The application of ocean colour data in coral reef areas is limited by the complexity of the water's optical properties in shallow coastal environments where they are found. The standard Case I algorithm for deriving chlorophyll concentration fail in turbid coastal waters resulting in over estimation of chlorophyll along most coastal areas (Morel and Belanger, 2006), even if due to terrestrial influence considerable enhancements of the algal biomass in these shallow zones is expected. Further, the standard algorithms for both water types were developed on the assumption of optically deep waters. Therefore in clear shallow bottoms that are highly complex or reflective as with the case in coral reefs and atolls, bottom reflection can induce an increase in marine reflectance, which is wrongly interpreted as ocean colour constituents (Boss and Zaneveld 2003). Given these problems, until special algorithms that take into account the complexity in coral reef areas are developed and incorporated in the standard processing chains of the current ocean colour satellites, the usefulness of ocean

colour data for coral reef applications will remain limited (Boss and Zaneveld 2003, Mumby et al. 2004).

To derive chlorophyll estimates taking into account these problems we carried out a series of analyses with ocean colour observations from the Sea-viewing Wide Field-of-view Sensor (SeaWiFS), Moderate Resolution Imaging Spectro-radiometer (MODIS), and Medium Resolution Imaging Spectrometer Instrument (MERIS) sensors (Appendix S2). The GlobColour processor at the European Space Agency's GlobColour project (<http://hermes.acri.fr/GlobColour>) was used to process Level 2 data from the three sensors to derive monthly level-3 binned products, including case I and case II chlorophyll concentrations with their respective flags, at a resolution 4.63 km at the equator ([http://www.GlobColour.info/products\\_description.html](http://www.GlobColour.info/products_description.html)). Data from all the three sensors were merged to derive case I Chlorophyll, while MERIS Case II algorithm was used to retrieve case II chlorophyll (Schroeder et al. 2007). These Level 3 outputs do not spatially differentiate the regions where each of the water types are relevant; therefore further analysis using turbidity flags is required to discern and merge regions with the different water types into a homogenous continuous layer (Morel and Belanger 2006). To achieve this, we used turbidity and depth flags (<30m) derived from the processing of level 2 products, in a logical expression designed to merge respective case I and case II regions in a given month, and further to exclude shallow water (<30m) pixels. Having masked shallower depths using the depth flags, we assumed similar water column properties in masked areas to those found in adjacent deeper (>30m) water pixels, and extrapolated the deeper water pixels to these areas. To achieve this for each layer, we applied 3x3 spatial interpolator, which calculates the median value of 8 pixels adjacent to the pixel being considered. In effect, pixels adjacent to the missing value maintained their original values while the missing pixel was assigned the resulting value from the interpolator (Maina et al. 2008). These monthly mean layers were then temporally aggregated for the long-term average. The following workflow was adopted to derive ocean colour products.

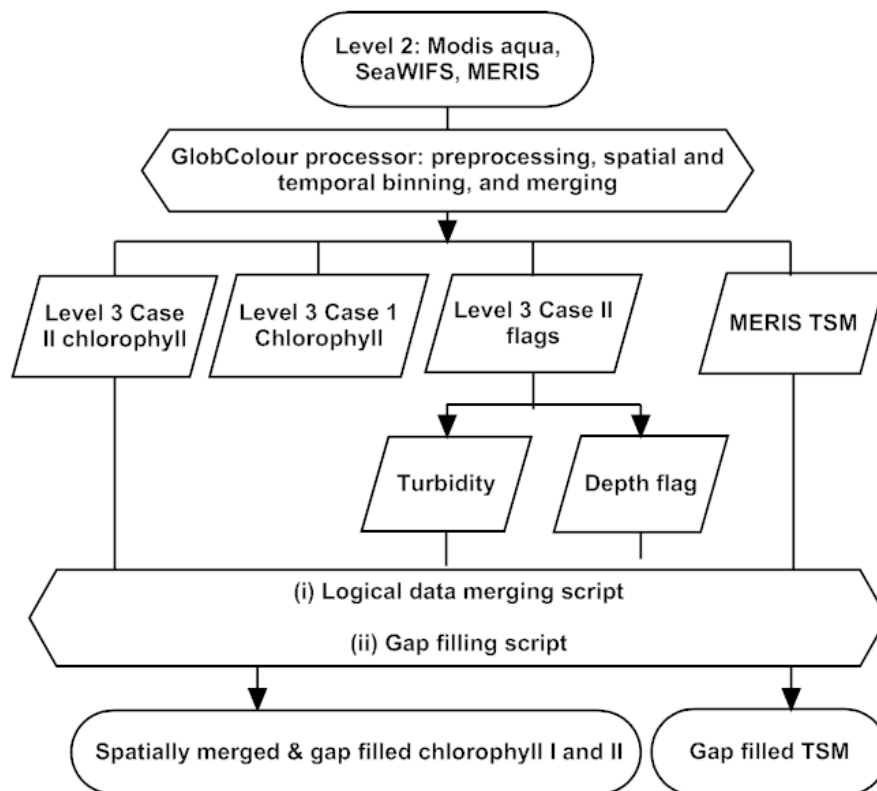


Figure 1. Figure showing the processing of the standard ocean colour products to enhance measurements for coastal areas.

**OC04a:** Time series - merged case I & II chlorophyll, CDOM and TSM

**OC04b:** Average Chlorophyll based on OC04a

**OC04c:** Average TSM based on OC04a

**OC04d:** Average CDOM based on OC04a

**Product OC05: Ocean acidification (based on pCO<sub>2</sub>, concentration under various IPCC SRES)**

\*\*\*\*\*Data not found\*\*\*\*\*

**Product OC06: UV 290-300nm**

Daily global maps of UV-erythemal (biologically damaging) irradiance at the Earth's surface (for the spectral range 290 to 400 nm and in the units of milli-watts m<sup>-2</sup>) in a 1 by 1.25 degree grid were retrieved for 1996 to 2001 from the NASA website (<http://toms.gsfc.nasa.gov>) (Herman et al. 1999, Vasilkov et al. 2001). This data is derived from the total ozone mapping spectrometer (TOMS) on-board Earth Probe-TOMS satellite. Erythemal radiation is a weighted average of UVA (315-400 nm) and UVB (280 to 315 nm) used as a measure of skin

irritation caused by exposure sunlight (Vasilkov et al. 2001). Errors associated with this data have not been ascertained for many parts of the world, however evaluations in Canada using a ground-based spectrometer reported absolute accuracy of 6% under normal conditions and 12% under conditions of UV absorbing aerosol plumes (Herman et al. 1999). These uncertainties are mostly influenced by the amount of ozone, clouds and aerosols, and terrain height. In the ocean, depth attenuation and the optical properties of the seawater influence the amount of radiation below water surface (Herman et al. 1999, Vasilkov et al. 2005). Radiative transfer modelling that includes the ocean system has been performed to estimate in-water radiation field (Vasilkov et al. 2005). Here we use Erythermal UV with no correction for the seawater optical properties. Previous reports have shown a good correlation of this data with coral bleaching where observations were made at varying depth (Maina et al. 2008).

The current online values of UV irradiance and Erythermal exposure from EP-TOMS have errors after 2001, and therefore can not be used for UV changes as these are more prone to time-dependent errors from cloud cover and aerosols. The application of this data here is limited to global mean, where the overall error is expected to be relatively small, as the mainly negative cloud-height errors and other positive errors usually partly cancel, leading to an overall smaller error (Liu et al. 2003). Consequently, UV average from 1997 to the end of 2001 was computed to represent local conditions in each grid square.

**OC06a:** Average Erythermal UV exposure

**LC01: Projected rainfall under IPCC SRES**

AOGCM (atmospheric-ocean global circulation models) were downloaded from three GCM data centres, for all the following IPCC scenarios: A1B [720ppm], A2 [870ppm] and B1 [550ppm]. A total of three models were obtained for a multi-model comparison.

**LC01a: CNRM model time series for A1b, A2, and B1**

**LC01b: NCAR model time series for A1b, A2, and B1**

## **LC01c: GISS model time series for A1b, A2, and B1**

### **OC07: Wind velocity and Doldrums Index**

Global sea surface wind speed ( $\text{ms}^{-1}$ ) estimates for 10 m above sea level at a 28-km resolution are available from the National Climatic Data Centre (NCDC, <ftp://eclipse.ncdc.noaa.gov/raid1b/seawinds>). NCDC wind data is based on the blended observations from multiple sensors, with reduced spatial and temporal gaps of individual satellite samplings, and reduced sub-sampling aliases and random errors (Zhang et al. 2006). Despite the coastal application of this data by the Coral Reef Watch, inter-comparisons with other products have not been performed because sparse in-situ measurements over the vast ocean surface make errors difficult to quantify (Zhang et al. 2006). Nonetheless, measurements from each sensor are passed through quality control prior to blending and gridding. Additionally, the blending of cross-calibrated multiple satellite observations is known to increase accuracy and resolution (Zhang et al. 2006, Zhang et al. 2009). Daily averaged wind speeds (2000-2009) and the averaged 10-year mean monthly wind speeds (1995-2004) were downloaded. The National Oceanic and Atmospheric Administration (NOAA) coral reef watch defines doldrums as wind conditions with a daily mean of less than  $3 \text{ m s}^{-1}$ . To estimate the magnitude and consistency of wind regimes in a given location, a doldrums metric was computed by taking the annual average maximum number of days that wind speeds were greater than  $3 \text{ m s}^{-1}$  over 10 years (2000-2009) and multiplying this by the 10-year mean monthly average.

**OC07a:** Long term wind velocity magnitude (windiness)

**OC07b:** Long term high wind velocity ( $>3\text{m/s}$ ) duration

**OC07c:** Doldrum index, as a function of OC07a and OC07b

**LE01:** Mangrove exposure to DoC - This product was developed in consultation with regional mangrove experts and is currently in preparation as a paper for publication. Several variables were utilized to derive the hydrologic, climatic and socioeconomic parameters, which influence the mangroves vulnerability to the drivers of change identified by the regional experts (Table 1). These drivers of change and their role in affecting the regional mangroves ecosystems are summarized in table 1. Data described in the following and previous sections were processed to derive variables, which were then used in Bayesian and fuzzy logic models to develop a spatial map of mangroves exposure to the drivers of ecosystem changes. The data and the steps followed are summarized in figure 2.

Table 1. Summary of variables identified by regional mangrove experts as important drivers of change for mangroves ecosystems and their roles in impacting mangroves.

Data/ derived Variable	Role in mangrove exposure to DoC
<b>Climate related</b>	
Historical land surface temperature	Areas where temperature is expected to significantly increase will experience aridity. This will increase salinities thus limiting or slowing mangrove growth
Precipitation	Most productive mangroves found in regions of high rainfall. High rainfall supports luxuriant mangrove growth. Arid areas tend to have stunted mangroves. The latter will thus be more vulnerable to CC related impacts as rainfall reduces
Sea level rise	Will inundate coastlines and thus submerge mangroves. Rate of inundation will vary depending on local geomorphology and SLR rate. Sea Level Anomaly was used as a proxy for sea level rise
Shoreline erosion	Will erode area occupied by mangroves leading to submergence of exposed areas
<b>Surface geomorphology</b>	
Elevation	Low lying areas will be more vulnerable to inundation/submergence due to SLR, while areas with relatively higher elevation will be less vulnerable
Slope	Will determine potential of mangroves to migrate landward. Steep slopes especially at the back of mangroves will hinder mangrove transgression. The contrary is true.
Species diversity	Areas with high species diversity will be less sensitive to environmental perturbations, and conversely true.
Coverage area	Areas with limited or low mangrove cover will be more vulnerable as areas suitable for mangrove growth shrink. Areas with wide stretches of intertidal areas will provide for large swathes for mangrove migration in response to SLR
Mangrove productivity	Mangroves exhibiting high productivity will more resilient to CC impacts e.g. reduced rainfall/increased aridity
<b>Other variables</b>	
Land cover land use/ Coastal development	Development in terms of infrastructure and even agriculture contiguous to mangroves will limit mangrove migration – no corridors for migration
Population density	Remote mangroves with limited access and thus low anthropogenic pressure will be more resilience to CC impacts
Rivers/fresh water influx	High river discharge ensures high nutrient input and moderated salinities. Also brings in sediments critical for accretion for mangroves to keep pace with SLR. Areas with limited or no freshwater discharge will be high vulnerable
<b>Soil type</b>	
Watershed susceptibility to erosion	Catchment degradation, steep slopes will enhance soil erosion and sedimentation downstream in which may smother mangroves causing dieback.

Mangrove Vulnerability Assessment	
CATEGORY	DATA
Land-use Intensity and Sediment	<ul style="list-style-type: none"> <li>• Land use intensity (LDI)</li> <li>• Watershed susceptibility to erosion</li> <li>• Soil (RUSLE)</li> </ul>
Human Disturbance Index	<ul style="list-style-type: none"> <li>• Population intensity</li> <li>• Poverty indices</li> </ul>
Geomorphology and Sea-level	<ul style="list-style-type: none"> <li>• Sea level anomaly (SLA)</li> <li>• Elevation</li> <li>• Land transgression [land use, slope]</li> </ul>
Ecological Condition	<ul style="list-style-type: none"> <li>• NDVI</li> </ul>

Figure 2. A flow chart showing the steps and data used to extract and synthesizing the variables into a mangrove exposure map.

**LE01a:** Distance to steep slope (calculated from LG01e)

**LE01b:** Watershed susceptibility to erosion (same product as described in LG01)

**LE01c:** Mangrove ecological condition – this product was calculated from the NDVI time series (see LE02). The Normalized Difference Vegetation Index (NDVI) is a good indicator of the presence of vegetation in the area of observation. In case of the present study, the MODIS 13 NDVI product of 16 day composites and at 250 m resolution was used. The data is stored as 16 bit signed integer but can be descaled to the original data range of 0 to 1.

**LE01d:** Human Pressure Index – this product was developed from a global population database and poverty metrics (<http://www.ciesin.org/>). It is a measure of population density or pressures to mangroves as a result of population density.

**LE01e:** Land Development Intensity index – An index of Landscape Development Intensity (LDI) was calculated for watersheds of varying sizes to estimate the potential impacts from human-dominated activities that are experienced by ecological systems within those watersheds using methods developed by Brown and Viva, 2005. The intended use of the LDI is as an index of the human disturbance gradient (the level of human induced impacts on the biological, chemical, and physical processes of surrounding lands or waters). Here, we used LDI as an indicator of human disturbance, and applied and used this as an input to mangrove exposure map.

**LE01f:** Exposure to land development and erosion – This is a composite between the watershed susceptibility to erosion (LG01a) and the land development intensity index (LE01e). This product shows spatially the gradient of exposure of mangroves ecosystems to land use and soil erosion in the respective watersheds.

**LE01g:** Exposure of mangroves to sea level rise – Monthly climatologies of sea level anomaly (SLA) maps were downloaded from [www.AVISO.org](http://www.AVISO.org). The maximum value of the 12 maps were calculated and used as a proxy for sea level rise. The values were extrapolated to land to overlay with the mangrove extent using a 3x3 filter. These were then standardized between zero and one to produce an exposure map to sea level rise.

**LE01h:** Mangrove exposure map - Mangrove exposure map was developed by synthesizing all the DoC's from LE01a-e.

**LE02. Mangrove extent and NDVI time series** – NDVI index was extracted from MODIS website. Mangrove extent for Madagascar and East Africa were used to extract MODIS monthly NDVI values from 2002-2011. The NDVI values within the mangrove extents were assumed to significantly represent the mangroves.

**LE02a.** Mangrove-NDVI time series (Monthly averages from 2000-2011)

**LE02b.** Mangrove extent shape-files for East Africa and Madagascar

**ME01: Coral exposure to DOC** - This product is based on a recent paper (Maina et al. 2011). This study combined global spatial gradients of coral exposure to radiation stress factors (temperature, UV light and doldrums), stress-reinforcing factors (sedimentation and eutrophication), and stress-reducing factors (temperature variability and tidal amplitude) to produce a global map of coral exposure and identify areas where exposure depends on factors that can be locally managed. A systems analytical approach was used to define interactions between radiation stress variables, stress reinforcing variables and stress reducing variables. Fuzzy logic and spatial ordinations were employed to quantify coral exposure to these stressors.

**MM01: ASCLME countries** – updated protected area polygons – to incorporate all type of closures e.g. new community closures in TZ, MQ and Kenya

Marine Protected Areas (MPA') from different sources at different scales are presented. A regional MPA map was derived from the global MPA database hosted at

<http://www.protectedplanet.net/>. This database does not incorporate some of the recent

additions to the MPA records in the Western Indian Ocean region. MPA maps from two countries, Kenya and Madagascar complete with the new protected areas are incorporated.

**MM02: Oil, gas and mineral prospecting and exploitation sites** - This product is available only for Madagascar, Efforts to obtain the similar maps for other countries in the region were not successful

## References

- Alcamo J, Schaldach R, Koch J, Kölking C, Lapola D, Priess J (2011) Evaluation of an integrated land use change model including a scenario analysis of land use change for continental Africa. *Environmental Modelling & Software*. 26:1017-1027.
- Brown MK, Vivas BM (2005) Landscape Development Intensity Index *Environmental Monitoring and Assessment*. 101: 289–309
- Boss E, Zaneveld JRV (2003) The Effect of Bottom Substrate on Inherent Optical Properties: Evidence of Biogeochemical Processes. *Limnology and Oceanography* 48: 346-354.
- Federer CA, Vörösmarty C, Fekete BM (2003) Sensitivity of Annual Evaporation to Soil and Root Properties in Two Models of Contrasting Complexity, *Journal of Hydrometeorology* 4: 1276-1289.
- Herman JR, Krotkov NA, Celarier E, Larko D, Labow G (1999) Distribution of UV radiation at the Earth's surface from TOMS-measured UV-backscattered radiances. *Geophysical Research Letters* 104: 12,059 –12,076.
- Jarvis A, Reuter HI, Nelson A, Guevara E (2008) Hole-filled seamless SRTMdata V4, International Centre for Tropical Agriculture (CIAT), available from <http://srtm.csi.cgiar.org>.
- Kilpatrick KA, Podesta GP, Evans R (2001) Overview of the NOAA/NASA Advanced Very High Resolution Radiometer Pathfinder algorithm for sea surface temperature and associated matchup database. *Journal of Geophysical Research-Oceans* 106: 9179-9197.
- Lehner B, Verdin K, Jarvis A (2008) New global hydrography derived from space borne elevation data. *Eos, Transactions, AGU* 89: 93–94.
- Le Provost C, Lyard F, Molines JM, Genco ML, Rabilloud F (1998) A hydrodynamic ocean tide model improved by assimilating a satellite altimeter-derived data set. *Geophysical Research Letters* 103: 5513-5529.

- Liu X, Newchurch MJ, Kim JH (2003) Occurrence of ozone anomalies over cloudy areas in TOMS version-7 level-2 data. *Atmospheric Chemistry and Physics* 3,187–223.
- Lyard F, Lefevre F, Letellier T, Francis O (2006) Modelling the global ocean tides: modern insights from FES2004. *Ocean Dynamics*, 56, 394–415.
- Maina J, Venus V, McClanahan TR, Ateweberhan M (2008) Modelling susceptibility of coral reefs to environmental stress using remote sensing data and GIS models in the western Indian Ocean. *Ecological Modelling* 212: 180-199.
- Maina J, McClanahan TR, Venus V, Ateweberhan M, Madin J (2011) Global gradients of coral exposure to environmental stresses and implications for local management. *PLoS ONE*. 6(8).
- Morel A, Prieur L (1977) Analysis of Variations in Ocean Colour. *Limnology and Oceanography* 22: 709-722.
- Morel A, Bélanger S (2006) Improved detection of turbid waters from ocean colour sensors information. *Remote Sensing of Environment* 102: 237-249.
- Mumby PJ, Skirving W, Strong AE, Hardy JT, LeDrew EF et al. (2004) Remote sensing of coral reefs and their physical environment. *Marine Pollution Bulletin* 48: 219.
- Nam PT, Yang D, Kanae S, Oki T, Musiak K (2003) Global soil loss estimate using rusle model: the use of global spatial dataset on estimating erosive parameters. *Geoinformatics* 14: 49-53.
- Renard KG, Freimund JR (1994) Using monthly precipitation data to estimate the R-factor in the revised USLE. *Journal of Hydrology* 157: 287-306.
- Schaldach R, Alcamo A, Koch J, Kölking C, Lapola DM, Schüngel J, Priess JA (2011) An integrated approach to modelling land-use change on continental and global scales. *Environmental Modelling & Software*. 26:1041-1051.
- Schroeder T, Behnert I, Schaale M, Fischer J, Doerffer R (2007) Atmospheric correction algorithm for MERIS above case-2 waters. *International Journal of Remote Sensing*. 28: 1469–1486.
- Selig ER, Casey KS, Bruno JF (2010) New insights into global patterns of ocean temperature anomalies: implications for coral reef health and management. *Global Ecology and Biogeography* 19: 397–411
- Vasilkov A, Krotkov N, Herman J., McClain CR., Arrigo K, et al. (2001) Global mapping of underwater UV irradiances and DNA-weighted exposures using Total Ozone Mapping Spectrometer and Sea-viewing Wide Field-of-view Sensor data products. *Geophysical Research Letters* 106: 27,205-27,219.

- Vasilkov AP, Herman JR, Ahmad Z, Kahru M, Mitchell BG (2005) Assessment of the ultraviolet radiation field in ocean waters from space-based measurements and full radiative-transfer calculations. *Applied Optics* 44: 2863-2869.
- Vörösmarty CJ, Federer CA, Schloss AL (1998) Potential evaporation functions compared on US watersheds: possible implications for global-scale water balance and terrestrial ecosystem modeling. *Journal of Hydrology*, 207: 147-169.
- Vrieling A, Sterk G, Jong SMD (2010) Satellite-based estimation of rainfall erosivity for Africa. *Journal of Hydrology*. 395: 235–241
- Zhang HM, Bates JJ, Reynolds RW (2006) Assessment of composite global sampling: Sea surface wind speed. *Geophysical Research Letters* 33: L17714.
- Zhang HM, Reynolds RW, Lumpkin R, Molinari R, Arzayus K, et al. (2009) An integrated global observing system for sea surface temperature using satellites and in situ data: Research to operations. *Bulletin of American Meteorological Society* 90: 31-38.